SLAC–PUB–6451
March 1994
(T/E)

Measurement of α_s from Energy-Energy Correlations at the Z^0 Resonance

K. Abe,[27] I. Abt,[13] W.W. Ash,[25]† D. Aston,[25] N. Bacchetta,[20] K.G. Baird,[23] C. Baltay,[31] H.R. Band,[30] M.B. Barakat,[31] G. Baranko,[9] O. Bardon,[16] T. Barklow,[25] A.O. Bazarko,[10] R. Ben-David,[31] A.C. Benvenuti,[2] T. Bienz,[25] G.M. Bilei,[21] D. Bisello,[20] G. Blaylock,[7] J.R. Bogart,[25] T. Bolton,[10] G.R. Bower,[25] J.E. Brau,[19] M. Breidenbach,[25] W.M. Bugg,[26] D. Burke,[25] T.H. Burnett,[29] P.N. Burrows,[16] W. Busza,[16] A. Calcaterra,[12] D.O. Caldwell,[6] D. Calloway,[25] B. Camanzi,[11] M. Carpinelli,[22] R. Cassell,[25] R. Castaldi,[22][a] A. Castro,[20] M. Cavalli-Sforza,[7] E. Church,[29] H.O. Cohn,[26] J.A. Coller,[3] V. Cook,[29] R. Cotton,[4] R.F. Cowan,[16] D.G. Coyne,[7] A. D'Oliveira,[8] C.J.S. Damerell,[24] S. Dasu,[25] R. De Sangro,[12] P. De Simone,[12] R. Dell'Orso,[22] Y.C. Du,[26] R. Dubois,[25] B.I. Eisenstein,[13] R. Elia,[25] C. Fan,[9] M.J. Fero,[16] R. Frey,[19] K. Furuno,[19] T. Gillman,[24] G. Gladding,[13] S. Gonzalez,[16] G.D. Hallewell,[25] E.L. Hart,[26] Y. Hasegawa,[27] S. Hedges,[4] S.S. Hertzbach,[17] M.D. Hildreth,[25] J. Huber,[19] M.E. Huffer,[25] E.W. Hughes,[25] H. Hwang,[19] Y. Iwasaki,[27] P. Jacques,[23] J. Jaros,[25] A.S. Johnson,[3] J.R. Johnson,[30] R.A. Johnson,[8] T. Junk,[25] R. Kajikawa,[18] M. Kalelkar,[23] I. Karliner,[13] H. Kawahara,[25] H.W. Kendall,[16] M.E. King,[25] R. King,[25] R.R. Kofler,[17] N.M. Krishna,[9] R.S. Kroeger,[26] Y. Kwon,[25] J.F. Labs,[25] M. Langston,[19] A. Lath,[16] J.A. Lauber,[9] D.W.G. Leith,[25] X. Liu,[7] M. Loreti,[20] A. Lu,[6] H.L. Lynch,[25] J. Ma,[29] G. Mancinelli,[21] S. Manly,[31] G. Mantovani,[21] T.W. Markiewicz,[25] T. Maruyama,[25] H. Masuda,[25] E. Mazzucato,[11] A.K. McKemey,[4] B.T. Meadows,[8] R. Messner,[25] P.M. Mockett,[29] K.C. Moffeit,[25] B. Mours,[25] G. Müller,[25] D. Muller,[25] T. Nagamine,[25] U. Nauenberg,[9] H. Neal,[25] M. Nussbaum,[8] L.S. Osborne,[16] R.S. Panvini,[28] H. Park,[19] T.J. Pavel,[25] I. Peruzzi,[12][b] L. Pescara,[20] M. Piccolo,[12] L. Piemontese,[11] E. Pieroni,[22] K.T. Pitts,[19] R.J. Plano,[23] R. Prepost,[30] C.Y. Prescott,[25] G.D. Punkar,[25] J. Quigley,[16] B.N. Ratcliff,[25] T.W. Reeves,[28] P.E. Rensing,[25] L.S. Rochester,[25] J.E. Rothberg,[29] P.C. Rowson,[10] J.J. Russell,[25] O.H. Saxton,[25]

T. Schalk,[7] R.H. Schindler,[25] U. Schneekloth,[16] B.A. Schumm,[15]
A. Seiden,[7] S. Sen,[31] M.H. Shaevitz,[10] J.T. Shank,[3] G. Shapiro,[15]
D.J. Sherden,[25] C. Simopoulos,[25] S.R. Smith,[25] J.A. Snyder,[31]
P. Stamer,[23] H. Steiner,[15] R. Steiner,[1] M.G. Strauss,[17] D. Su,[25]
F. Suekane,[27] A. Sugiyama,[18] S. Suzuki,[18] M. Swartz,[25] A. Szumilo,[29]
T. Takahashi,[25] F.E. Taylor,[16] E. Torrence,[16] J.D. Turk,[31] T. Usher,[25]
J. Va'Vra,[25] C. Vannini,[22] E. Vella,[29] J.P. Venuti,[28] P.G. Verdini,[22]
S.R. Wagner,[25] A.P. Waite,[25] S.J. Watts,[4] A.W. Weidemann,[26]
J.S. Whitaker,[3] S.L. White,[26] F.J. Wickens,[24] D.A. Williams,[7]
D.C. Williams,[16] S.H. Williams,[25] S. Willocq,[31] R.J. Wilson,[3]
W.J. Wisniewski,[5] M. Woods,[25] G.B. Word,[23] J. Wyss,[20]
R.K. Yamamoto,[16] J.M. Yamartino,[16] S.J. Yellin,[6] C.C. Young,[25]
H. Yuta,[27] G. Zapalac,[30] R.W. Zdarko,[25] C. Zeitlin,[19] and J. Zhou,[19]

(The SLD Collaboration)

[1] *Adelphi University, Garden City, New York 11530*
[2] *INFN Sezione di Bologna, I-40126 Bologna, Italy*
[3] *Boston University, Boston, Massachusetts 02215*
[4] *Brunel University, Uxbridge, Middlesex UB8 3PH, United Kingdom*
[5] *California Institute of Technology, Pasadena, California 91125*
[6] *University of California at Santa Barbara, Santa Barbara, California 93106*
[7] *University of California at Santa Cruz, Santa Cruz, California 95064*
[8] *University of Cincinnati, Cincinnati, Ohio 45221*
[9] *University of Colorado, Boulder, Colorado 80309*
[10] *Columbia University, New York, New York 10027*
[11] *INFN Sezione di Ferrara and Università di Ferrara, I-44100 Ferrara, Italy*
[12] *INFN Lab. Nazionali di Frascati, I-00044 Frascati, Italy*
[13] *University of Illinois, Urbana, Illinois 61801*
[14] *KEK National Laboratory, Tsukuba-shi, Ibaraki-ken 305 Japan*
[15] *Lawrence Berkeley Laboratory, University of California, Berkeley, California 94720*
[16] *Massachusetts Institute of Technology, Cambridge, Massachusetts 02139*
[17] *University of Massachusetts, Amherst, Massachusetts 01003*
[18] *Nagoya University, Chikusa-ku, Nagoya 464 Japan*
[19] *University of Oregon, Eugene, Oregon 97403*
[20] *INFN Sezione di Padova and Università di Padova, I-35100 Padova, Italy*
[21] *INFN Sezione di Perugia and Università di Perugia, I-06100 Perugia, Italy*
[22] *INFN Sezione di Pisa and Università di Pisa, I-56100 Pisa, Italy*

[23] *Rutgers University, Piscataway, New Jersey 08855*
[24] *Rutherford Appleton Laboratory, Chilton, Didcot, Oxon OX11 0QX United Kingdom*
[25] *Stanford Linear Accelerator Center, Stanford University, Stanford, California 94309*
[26] *University of Tennessee, Knoxville, Tennessee 37996*
[27] *Tohoku University, Sendai 980 Japan*
[28] *Vanderbilt University, Nashville, Tennessee 37235*
[29] *University of Washington, Seattle, Washington 98195*
[30] *University of Wisconsin, Madison, Wisconsin 53706*
[31] *Yale University, New Haven, Connecticut 06511*
[†] *Deceased*
[a] *Also at the Università di Genova*
[b] *Also at the Università di Perugia*

ABSTRACT

We have determined the strong coupling α_s from a comprehensive study of energy-energy correlations (EEC) and their asymmetry ($AEEC$) in hadronic decays of Z^0 bosons collected by the SLD experiment at SLAC. The data were compared with all four available predictions of QCD calculated up to $\mathcal{O}(\alpha_s^2)$ in perturbation theory, and also with a resummed calculation matched to all four of these calculations. We find large discrepancies between α_s values extracted from the different $\mathcal{O}(\alpha_s^2)$ calculations. We also find a large renormalization scale ambiguity in α_s determined from the EEC using the $\mathcal{O}(\alpha_s^2)$ calculations; this ambiguity is reduced in the case of the $AEEC$, and is very small when the matched calculations are used. Averaging over all calculations, and over the EEC and $AEEC$ results, we obtain $\alpha_s(M_Z^2) = 0.124^{+0.003}_{-0.004}(exp.) \pm 0.009(theory)$.

Submitted to Physical Review D.

This work was supported by Department of Energy contracts: DE-FG02-91ER40676 (BU), DE-FG03-92ER40701 (CIT), DE-FG03-91ER40618 (UCSB), DE-FG02-91ER40672 (Colorado), DE-FG02-91ER40677 (Illinois), DE-AC03-76SF00098 (LBL), DE-FG02-92ER40715 (Massachusetts), DE-AC02-76ER03069 (MIT), DE-FG06-85ER40224 (Oregon), DE-AC03-76SF00515 (SLAC), DE-FG05-91ER40627 (Tennessee), DE-AC02-76ER00881 (Wisconsin), DE-FG02-92ER40704 (Yale); National Science Foundation grants: PHY-91-13428 (UCSC), PHY-89-21320 (Columbia), PHY-92-04239 (Cincinnati), PHY-88-17930 (Rutgers), PHY-88-19316 (Vanderbilt), PHY-92-03212 (Washington); the UK Science and Engineering Research Council (Brunel and RAL); the Istituto Nazionale di Fisica Nucleare of Italy (Bologna, Ferrara, Frascati, Pisa, Padova, Perugia); the Natural Sciences and Engineering Research Council of Canada (British Columbia, Victoria, TRIUMF); and the Japan-US Cooperative Research Project on High Energy Physics (Nagoya, Tohoku).

I. INTRODUCTION

Measurement of the strong coupling α_s in various hard processes and at different hard scales is one of the crucial tests of Quantum Chromodynamics (QCD) [1]. In e^+e^- annihilation α_s may be determined from inclusive measures of the topology of hadronic events. We have previously determined α_s from the rate of multijet events in hadronic decays of Z^0 bosons collected by the SLD experiment at SLAC [2]. We found $\alpha_s = 0.118 \pm 0.002(stat.) \pm 0.003(syst.) \pm 0.010(theory)$, where the dominant uncertainty arises from uncalculated higher order contributions in perturbation theory. Here we present complementary measurements of α_s using energy-energy correlations (EEC) and the asymmetry of energy-energy correlations ($AEEC$) [3]. These are inclusive two-particle correlations that can be used to probe the structure of hadronic events in more detail than the event topology variables and can be calculated perturbatively in QCD. Comparison of α_s determined in this way with that measured from event topology variables provides a significant consistency check of the validity of perturbative QCD.

The EEC is defined as the normalized energy-weighted sum over all pairs of particles whose opening angles χ_{ij} lie between $\chi - \Delta\chi/2$ and $\chi + \Delta\chi/2$:

$$EEC(\chi) = \frac{1}{N_{event}} \sum_{1}^{N_{event}} \left(\frac{1}{\Delta\chi} \int_{\chi-\frac{\Delta\chi}{2}}^{\chi+\frac{\Delta\chi}{2}} \sum_{i,j=1}^{n_{particle}} \frac{E_i E_j}{E_{vis}^2} \delta(\chi' - \chi_{ij}) d\chi' \right), \qquad (1)$$

where χ is an opening angle to be studied for the correlations; $\Delta\chi$ is a bin width; E_i and E_j are the energies of particles i and j and E_{vis} is the sum of the energies of all particles in the event. In the central region, $\chi \sim 90°$, the shape of the EEC is determined by hard gluon emission; hadronization contributions are expected to

be large in the collinear and back-to-back regions, $\chi \sim 0^\circ$ and 180° respectively. The asymmetry of the EEC is defined as

$$AEEC(\chi) = EEC(\pi - \chi) - EEC(\chi). \tag{2}$$

Perturbative QCD calculations of the EEC were first performed up to $\mathcal{O}(\alpha_s^2)$ in 1983 by Richards, Stirling and Ellis (RSE) [4]. Since then similar calculations have been performed by Ali and Barreiro (AB) [5], Falck and Kramer (FK) [6], and Kunszt and Nason (KN) [7]. These calculations, valid in the central region, have the general form

$$EEC(\chi) = \frac{\alpha_s(\mu^2)}{2\pi} A(\chi) + \left(\frac{\alpha_s(\mu^2)}{2\pi}\right)^2 \left[A(\chi) 2\pi b_0 \ln(\mu^2/s) + B(\chi)\right], \tag{3}$$

where, to the same order in perturbation theory, $\alpha_s(\mu^2)$ is related to the QCD scale $\Lambda_{\overline{MS}}$ by [8]

$$\alpha_s(\mu^2) = \frac{1}{b_0 \ln(\mu^2/\Lambda^2_{\overline{MS}})} \left[1 - \frac{b_1}{b_0^2} \frac{\ln\left[\ln(\mu^2/\Lambda^2_{\overline{MS}})\right]}{\ln(\mu^2/\Lambda^2_{\overline{MS}})}\right]; \tag{4}$$

μ is the renormalization scale, often expressed in terms of the factor $f = \mu^2/s$; $\sqrt{s}$ is the center-of-mass energy of the experiment; $b_0 = (33 - 2n_f)/12\pi$; $b_1 = (153 - 19n_f)/29\pi^2$; and n_f is the number of active quark flavors. Here we have assumed the definition of $\Lambda_{\overline{MS}}$ for five active flavors. The first order coefficients $A(\chi)$ can be calculated analytically and the second order coefficients $B(\chi)$ are calculated numerically. The main difference between the four theoretical calculations mentioned above is in the method used to treat the singularities appearing in the second order coefficients in the angular regions $\chi \sim 0^\circ$ and $\sim 180^\circ$.

It is important to note that $\mathcal{O}(\alpha_s^2)$ perturbative QCD calculations do not specify the μ value to be used for any physical observable, although this scale ambiguity will presumably vanish if the calculation is done to all orders in perturbation theory. Large scale ambiguities in determinations of α_s using such calculations for the EEC and event variables have been reported [2,9–11]. There is an indication that the $AEEC$ may be less sensitive to higher-order perturbative QCD contributions than the EEC [4], and may therefore be expected to be less sensitive to changes of renormalization scale. One also expects *a priori* that non-perturbative hadronization effects will tend to cancel in the $AEEC$.

Furthermore, discrepancies between the four $\mathcal{O}(\alpha_s^2)$ calculations of the EEC have been reported [11]. These discrepancies between calculations each supposedly complete to $\mathcal{O}(\alpha_s^2)$ are not understood, but may be interpreted as an indication that not all $\mathcal{O}(\alpha_s^2)$ terms have been included in some or all of the calculations. In the absence of further information we assume that all calculations are equally valid and use them all in our determination of α_s, taking the spread in α_s values as an indication of calculation uncertainty.

Recently progress has been made in perturbative QCD in the form of 'resummed' calculations of certain event shape measures in e^+e^- annihilation [12]. These techniques have been used [13,14] to calculate the EEC in the back-to-back region, where a large contribution from soft and collinear gluon radiation appears, by exponentiating the leading and next-to-leading order terms in $L \equiv \ln(1/y)$, where $y = \frac{1+\cos\chi}{2}$, up to all orders† in α_s . Within this formalism the cumulative EEC can be written [13]

† Earlier work on a perturbative evaluation of the leading and next-to-leading order terms in L of the EEC was performed up to two-loop level by Collins and Soper [15].

$$R_{EEC}(y) \equiv \int_0^y EEC(y')dy' = \Big(1 + \sum_{n=1}^{\infty} \alpha_s^n C_n\Big)\Sigma(y,\alpha_s) + \sum_{n=1}^{\infty} \alpha_s^n Y_n(y), \qquad (5)$$

where

$$\begin{aligned}
\ln(\Sigma(y,\alpha_s)) &= \sum_{n=1}^{\infty} \alpha_s^n \sum_{m=1}^{n+1} G_{nm} \ln^m(1/y) \\
&= (\quad G_{12}L^2 \quad + \quad G_{11}L \quad) \quad \alpha_s \\
&+ (\quad G_{23}L^3 \quad + \quad G_{22}L^2 \quad + \quad G_{21}L \quad) \quad \alpha_s^2 \\
&+ \quad \cdots \\
&= \underline{Lg_1(\alpha_s L)} \quad + \quad \underline{g_2(\alpha_s L)} \quad + \quad \underline{\alpha_s g_3(\alpha_s L) + \cdots}\ ; \qquad (6) \\
&\qquad \text{Leading} \qquad \text{Next-to-leading} \qquad \text{Subleading}
\end{aligned}$$

C_n and G_{nm} are constants; $Y_n(y)$ are functions which vanish as $y \to 0$; and the functions g_1 and g_2 are the sums of the leading and next-to-leading logarithms in L, respectively. Except for the term proportional to G_{21}, which can be estimated from the $\mathcal{O}(\alpha_s^2)$ calculations, the subleading terms have not been calculated. An analytic evaluation of the EEC singularity structure [13] gives an approximate simplified form:

$$R_{EEC}^{resum}(y) = (1 + C_1\alpha_s)\exp\big(Lg_1(\alpha_s L) + g_2(\alpha_s L)\big). \qquad (7)$$

This resummed calculation can be combined with each of the $\mathcal{O}(\alpha_s^2)$ calculations, also expressed in the cumulative form:

$$R_{EEC}^{\mathcal{O}(\alpha_s^2)}(y) = 1 + \mathcal{A}(y)\alpha_s + \mathcal{B}(y)\alpha_s^2, \qquad (8)$$

where $\mathcal{A}$ and $\mathcal{B}$ are the cumulative forms of A and B in Eq. (3). Subtracting double-counted terms yields the *matched* form:

$$R_{EEC}^{match}(y) = R_{EEC}^{resum}(y) + R_{EEC}^{\mathcal{O}(\alpha_s^2)}(y) - (C_1 + G_{11}L + G_{12}L^2)\alpha_s \qquad (9)$$
$$- \left[G_{22}L^2 + G_{23}L^3 + (G_{11}L + G_{12}L^2)\big(C_1 + \frac{1}{2}(G_{11}L + G_{12}L^2)\big)\right]\alpha_s^2.$$

This procedure is called the '*R-matching*' scheme.† Equation (9) can be differentiated with respect to χ and compared with the data. A '*modified R-matching*' scheme is also proposed in Ref. [13], whereby the subleading term proportional to G_{21} at $\mathcal{O}(\alpha_s^2)$ (Eq. (6)) is included in the argument of the exponential in Eq. (9). It can be argued that *modified R-matching* is preferred theoretically [17] because the extra subleading term at $\mathcal{O}(\alpha_s^2)$ is explicitly exponentiated.

In this analysis we attempt to be as comprehensive as possible and compare all four $\mathcal{O}(\alpha_s^2)$ calculations with data in the central region to determine α_s. We then combine the resummed calculation with all four of the fixed order calculations, using both the *R-matching* and *modified R-matching* schemes, to make an improved determination of α_s. We study in particular the dependence of α_s on the QCD renormalization scale, which is expected *a priori* to be weaker when the resummed calculation is used. We compare our results with α_s measured from our jet rates analysis [2] and with measurements from LEP [9–11,16,18–22].

† Another scheme, '*lnR-matching*', has also been proposed [12] to combine the resummed and $\mathcal{O}(\alpha_s^2)$ calculations for event shape variables, but it cannot be applied reliably to the EEC [16].

II. THE SLD AND EVENT SELECTION

The data used in this analysis were recorded in 1992 by the SLC Large Detector (SLD) [23] from electron-positron annihilation events at the Z^0 resonance produced by the SLAC Linear Collider (SLC). A subset of the components of the SLD is used for this analysis. Charged particles are tracked in the vertex detector (VXD) [24] and in the Central Drift Chamber (CDC) [23]. Momentum measurement is provided by a uniform axial magnetic field of 0.6 T. Particle energies are measured in the Liquid Argon Calorimeter (LAC) [25], which contains both electromagnetic and hadronic sections, and in the Warm Iron Calorimeter [26]. In this analysis the calorimeters are used only for triggering and event selection.

Three triggers were used for hadronic events, one requiring a total LAC electromagnetic energy greater than 30 GeV, another requiring at least two well-separated tracks in the CDC, and a third requiring at least 8 GeV in the LAC and one track in the CDC. A selection of hadronic events was then made by two independent methods, one based on the topology of energy depositions in the calorimeters, the other on the number and topology of charged tracks measured in the CDC.

The analysis presented here used charged tracks measured in the CDC and VXD. A set of cuts was applied to the data to select well-measured tracks and events well-contained within the detector acceptance. Tracks were required to have: (1) a distance from the measured interaction point, at the point of closest approach, of less than 5 cm in the direction transverse to the beam axis and 10 cm along the beam axis; (2) a polar angle θ with respect to the beam axis within $|\cos\theta| < 0.80$; (3) a momentum transverse to the beam axis of $p_\perp > 150$ MeV/c.

Events were required to have: (1) a minimum of five such tracks; (2) a total visible energy calculated from the selected tracks of at least 20 GeV; (3) a thrust axis [27] direction within $|\cos\theta_T| < 0.71$. From our 1992 data sample 6476 events survived these cuts. The efficiency for selecting hadronic events satisfying the $|\cos\theta_T|$ cut is estimated to be above 96%. The background in the selected event sample is estimated to be $0.3\pm0.1\%$, dominated by $Z^0 \to \tau^+\tau^-$ events. Distributions of single particle and event topology observables in the selected events are found to be well described by Monte Carlo models of hadronic Z^0 boson decays [28,29] combined with a simulation [30] of the SLD.

III. MEASUREMENT OF *EEC* AND *AEEC*

The EEC was calculated using all pairs of selected charged tracks, assigning each the charged pion mass. Figure 1 shows the measured EEC and $AEEC$. The bin width was chosen to be 3.6°, which is much larger than the two-particle angular resolution of the detector, so as to minimize bin-to-bin migration effects in the data correction procedure to be described later. Also shown in Fig. 1 are comparisons with the JETSET [28] and HERWIG [29] Monte Carlo programs which simulate the hadronic decays of Z^0 bosons, combined with a simulation of the SLD, and the same event reconstruction and selection procedures as applied to the data. For each program 100,000 events were generated. For JETSET we used parameter values determined by the TASSO Collaboration at $\sqrt{s} = 35$ GeV [31], which have been found to be in good agreement with Z^0 data [32]. For HERWIG we used the default parameter values which were derived from comparisons with LEP data [33]. Both simulations reproduce the general features of the data.

We used both JETSET and HERWIG simulations to correct our data for the effects of initial state photon radiation, detector acceptance and resolution, interactions and decays in the detector, analysis cuts, and unmeasured neutral particles. The measured EEC, $EEC_{meas}(\chi_i)$, was corrected to the *hadron level*, $EEC_{hadron}(\chi_i)$, by applying bin-by-bin correction factors, $C_{det}^{EEC}(\chi_i)$:

$$EEC_{hadron}(\chi_i) = C_{det}^{EEC}(\chi_i) \times EEC_{meas}(\chi_i), \tag{10}$$

where the correction factors were calculated by comparing Monte Carlo results before and after detector simulation:

$$C_{det}^{EEC}(\chi_i) = \frac{EEC_{hadron}^{MC}(\chi_i)}{EEC_{detector}^{MC}(\chi_i)}, \tag{11}$$

where $EEC_{detector}^{MC}(\chi_i)$ represents the histogram content at bin χ_i of the EEC obtained from the charged particles of the reconstructed Monte Carlo events, and $EEC_{hadron}^{MC}(\chi_i)$ represents that from all the stable particles with lifetimes greater than 3×10^{-10} s in the generated Monte Carlo events with no initial state photon radiation. The corrected $AEEC$ was then derived from the corrected EEC. Systematic errors in this correction procedure will be discussed later.

We corrected the data further for the effects of hadronization using both JETSET and HERWIG. The *parton-level* EEC is defined by

$$EEC_{parton}(\chi_i) = C_{frag}^{EEC}(\chi_i) \times EEC_{hadron}(\chi_i), \tag{12}$$

where the correction factor $C_{frag}^{EEC}(\chi_i)$ is defined by

$$C_{frag}^{EEC}(\chi_i) = \frac{EEC_{parton}^{MC}(\chi_i)}{EEC_{hadron}^{MC}(\chi_i)}, \tag{13}$$

where $EEC^{MC}_{hadron}(\chi_i)$ is the hadron-level EEC as defined in Eq. (11), and $EEC^{MC}_{parton}(\chi_i)$ is the content of bin χ_i constructed at the parton level.† The corrected $AEEC$ was again derived from the corrected EEC.

The parton-level EEC and $AEEC$ are shown in Figs. 2(a) and 3(a) respectively, where JETSET was used for both the detector and hadronization corrections. The correction factors for the EEC for detector effects and hadronization effects are shown in Figs. 2(b) and (c) respectively. Figures 3(b) and (c) show the corresponding effective correction factors for the $AEEC$, which are defined as $C^{AEEC}_{det}(\chi_i) = AEEC^{MC}_{hadron}(\chi_i)/AEEC^{MC}_{det}(\chi_i)$ and $C^{AEEC}_{frag}(\chi_i) = AEEC^{MC}_{parton}(\chi_i)/AEEC^{MC}_{hadron}(\chi_i)$ respectively. Also shown in Figs. 2(b) and (c), and Figs. 3(b) and (c) are the correction factors calculated using HERWIG. It is interesting to note that JETSET and HERWIG give slightly different correction factors in the central region of the EEC (Figs. 2(b) and (c)), although both describe the detector-level data well (Fig. 1(a)). We have found that this is due to differences in the relative production of charged and neutral particles, which also lead to the small differences seen in Fig. 1. However, the overall corrections to the parton level are found to be very similar in the central region. The differences between the JETSET and HERWIG correction factors will be discussed in the section on systematic errors (Section IV). It is also interesting that, despite the *a priori* expectation that hadronization effects should cancel in the $AEEC$, the magnitude of the deviation of the hadronization correction factors from unity is comparable for the $AEEC$ and EEC.

† The parton level is defined in JETSET by the parameter Q_0, which was set to 1 GeV, and in HERWIG by the parameter Q_g, which was set to 0.75 GeV.

The statistical errors on the EEC and $AEEC$ have strong bin-to-bin correlations because each track in each event contributes to several bins. The statistical error in each bin was estimated by taking the rms of the contents of that bin over ten Monte Carlo samples, each with the same number of events as the data sample. These errors were used in the fits below.

IV. DETERMINATION OF α_s

A. Determination of α_s using $\mathcal{O}(\alpha_s^2)$ calculations

We first determine α_s by comparing the four $\mathcal{O}(\alpha_s^2)$ QCD calculations with the parton-level EEC and $AEEC$ derived from the data. Each calculation was fitted to the fully corrected measured EEC and $AEEC$ by minimizing χ^2 under variation of $\Lambda_{\overline{MS}}$ for fixed renormalization scale factor f. The fits were restricted to the angular region $36^\circ \leq \chi \leq 154.8^\circ$ for the EEC and $21.6^\circ \leq \chi \leq 79.2^\circ$ for the $AEEC$, the ranges being chosen in such a way that (1) the uncertainty on the hadronization corrections is smaller than 30%, (see Figs. 2(c) and 3(c)), (2) the perturbation series for the EEC and the $AEEC$ remain reasonably convergent for all four QCD calculations [34], and (3) the fit quality at $f = 1$ is reasonable, $\chi^2_{dof} < 5$, where χ^2_{dof} is the χ^2 per degree of freedom of the fit.

Figures 2(a) and 3(a) show the results of the four $\mathcal{O}(\alpha_s^2)$ QCD fits with renormalization scale factor $f = 1$, to the EEC and $AEEC$ respectively. Figures 4(a) and 5(a) show $\alpha_s(M_Z^2)$, derived from the fitted $\Lambda_{\overline{MS}}$ for different values of f, using the EEC and $AEEC$ respectively. The corresponding fit quality χ^2_{dof} is shown in Figs. 4(b) and 5(b). In order to estimate the statistical errors on α_s we made use of the previously generated ten sets of Monte Carlo events.

We performed the same fitting procedure to the EEC and the $AEEC$ for each of these sets and took the rms deviation of the ten α_s values thus determined to be the statistical error of the fitted α_s (see Figs. 4(a) and 5(a)).

From Figs. 4 and 5 several features of the fit results are common to each QCD calculation: (1) $\alpha_s(M_Z^2)$ depends strongly on f, the dependence being stronger for the EEC than for the $AEEC$; (2) at low f the fit quality deteriorates rapidly, and neither α_s nor its error can be interpreted meaningfully; (3) the fits are relatively good in the scale range $f \gtrsim 2\times10^{-3}$ for the EEC and $f \gtrsim 5\times10^{-2}$ for the $AEEC$, and there is no strong preference for a particular scale. Similar features were seen in our α_s measurement from jet rates [2]. It should be noted that a comparison of α_s results from the various calculations at any particular scale f reveals systematic differences of up to 20% in magnitude,† although for the $AEEC$ the three more recent calculations are in reasonable agreement for $f > 0.01$.

Figures 4 and 5 represent a complete summary of our results. However, in order to quote a single value of α_s from each QCD calculation we adopt the following procedure. We consider the ranges $0.002 \leq f \leq 4$ for the EEC and $0.01 \leq f \leq 4$ for the $AEEC$. The lower bounds ensure that the perturbation series for the EEC and $AEEC$ remain reasonably convergent for all four QCD calculations [34] and that the fit quality is reasonable. The upper bound restricts μ to a reasonable physical region, $\mu \leq 2\ \overline{s}$. We take the extrema of the α_s values in these ranges to define the scale uncertainty. Table 1 summarizes the measured α_s, defined as the midpoint of α_s between the extrema, and the scale uncertainty, defined as the difference between the extrema and the midpoint value.

† This has also been observed previously [11].

The experimental systematic errors, which arise from uncertainties in modeling the acceptance, efficiency, and resolution of the detector, are summarized in Table 2. The largest contribution is from the understanding of the effects of our track and event selection cuts, which we evaluate by varying the cuts over wide ranges. We also varied the tracking efficiency and resolution by large amounts in our Monte Carlo simulations to account for any possible biases. In addition, the change in α_s is negligible when bins at either end of the fit range are removed. Effects due to limited Monte Carlo statistics are relatively small compared with the other errors. Total experimental systematic errors on α_s are estimated to be $^{+0.002}_{-0.003}$ for the EEC and ± 0.004 for the $AEEC$.

The theoretical uncertainties in parton production and hadronization were estimated by recalculating the hadronization correction factors using JETSET with values of Q_0 in the range 0.5–4.0 GeV,† and by using HERWIG, which contains a different hadronization model. The uncertainties in the correction factors are shown in Figs. 2(c) (EEC) and 3(c) ($AEEC$). The estimated hadronization uncertainties in α_s are ± 0.002 for the EEC and $^{+0.003}_{-0.002}$ for the $AEEC$.‡

The theoretical uncertainties from the numerical precision of the coefficients $A(\chi)$ and $B(\chi)$ in Eq. (3) are found to be negligible for all four QCD calculations.

Averaging over all four $\mathcal{O}(\alpha_s^2)$ QCD calculations to quote a single α_s value from each of the EEC and $AEEC$ analyses, we calculated the mean and rms deviation of the four α_s values at each f in the ranges shown in Figs. 4 and 5, respectively. The central value of α_s was taken as the midpoint of α_s in that f range; the

† Differences observed for changes of the other main fragmentation parameters in JETSET, σ_q, a and b, are small and negligible compared to those of Q_0.

‡ These should be compared with overall shifts in $\alpha_s(M_Z^2)$ of $+0.014$ (EEC) and -0.015 ($AEEC$) due to the hadronization corrections.

calculation uncertainty was taken as the *rms* at the central value; and the *scale uncertainty* was taken as the difference between the central value and the extrema. We obtain:

$$EEC : \alpha_s(M_Z^2) = 0.127 \pm 0.001(stat.)^{+0.002}_{-0.003}(syst.) \pm 0.013(theory)$$

$$AEEC : \alpha_s(M_Z^2) = 0.116 \pm 0.002(stat.) \pm 0.004(syst.) \pm 0.006(theory).$$

The total theoretical uncertainty is the sum in quadrature of contributions from hadronization (± 0.002 for EEC, $^{+0.003}_{-0.002}$ for $AEEC$), calculation ($\pm$ 0.006 for EEC, $\pm$ 0.004 for $AEEC$), and scale ($\pm$ 0.011 for EEC, $\pm$ 0.003 for $AEEC$) uncertainties. These α_s values are in agreement with our measurement from jet rates [2]. They are also in agreement within experimental errors with α_s measurements from the EEC and $AEEC$ by other groups [9–11,18]. A large theoretical uncertainty, dominated by the scale uncertainty, was also found in our α_s measurement from jet rates [2] and is related to uncalculated higher order terms in QCD perturbation theory. The scale uncertainty for the $AEEC$ is smaller than that for the EEC, perhaps indicating that the contribution from uncalculated higher order terms is smaller in the former case as discussed in Section I. Finally, the discrepancy in α_s between the four calculations is a significant contribution to the total uncertainty for the EEC, and the dominant contribution for the $AEEC$.

B. Comparison of $\mathcal{O}(\alpha_s^2)$ and $\mathcal{O}(\alpha_s^2)$+resummed calculations

We now compare the $\mathcal{O}(\alpha_s^2)$ calculations with the matched $\mathcal{O}(\alpha_s^2)$+resummed calculations. For illustration we use the KN $\mathcal{O}(\alpha_s^2)$ calculation and the *modified R-matching* scheme. For this purpose we perform fits to the EEC data within the angular range $90^\circ \leq \chi \leq 154.8^\circ$, where the lower limit is the kinematic limit

for the resummed calculation and the upper limit is the same as in the previous section. Figure 6 shows the results of $\mathcal{O}(\alpha_s^2)$ and matched fits, with $f = 1$, to the parton-level corrected EEC. At $f = 1$, $\alpha_s(M_Z^2) = 0.126 \pm 0.002(stat.)$ with $\chi^2_{dof} = 1.86$ for the $\mathcal{O}(\alpha_s^2)$ fit, and $\alpha_s(M_Z^2) = 0.133 \pm 0.002(stat.)$ with $\chi^2_{dof} = 0.71$ for the matched fit. However, the $\mathcal{O}(\alpha_s^2)$ calculation cannot describe the large angle region $\chi \gtrsim 150°$, while the matched calculation describes the data even up to $\chi \sim 170°$. We show in addition in Fig. 6 a fit of the $\mathcal{O}(\alpha_s^2)$ calculation with $f = 0.0033$, which results in $\alpha_s(M_Z^2) = 0.114 \pm 0.001(stat)$ with $\chi^2_{dof} = 0.66$. With this small scale choice the $\mathcal{O}(\alpha_s^2)$ calculation describes the data up to $\chi \sim 165°$. This illustrates that an $\mathcal{O}(\alpha_s^2)$ calculation used with a small scale is able to reproduce, to some extent, the effects of the resummed logarithms in the matched calculation. However, the small scale choice results in a smaller fitted value of $\alpha_s(M_Z^2)$ than the choice $f = 1$.

Figure 7 shows the resulting $\alpha_s(M_Z^2)$ and χ^2_{dof} values for fits of the $\mathcal{O}(\alpha_s^2)$ and matched calculations at various values of f. It is apparent that good fits to the data can only be obtained for $f \gtrsim 10^{-3}$ ($\mathcal{O}(\alpha_s^2)$) or $f \gtrsim 0.2$ (matched).† Within the range $f \gtrsim 0.2$ the scale dependence of the matched calculation is significantly smaller than that of the $\mathcal{O}(\alpha_s^2)$ calculation, confirming the *a priori* expectation discussed in Section I.

† Similar results were obtained in our measurement of α_s from jet rates [2].

C. Determination of α_s using $\mathcal{O}(\alpha_s^2)$+resummed calculations

In this section we apply both the *R-matching* and *modified R-matching* schemes (see Section I) to combine the resummed calculation with each of the four $\mathcal{O}(\alpha_s^2)$ calculations of the EEC, and perform fits to the data. Note that such matched calculations cannot be applied to the $AEEC$ because no resummed calculation is available in the forward region, $0^\circ \leq \chi \leq 90^\circ$.

Figure 8 shows the results of the KN $\mathcal{O}(\alpha_s^2)$+resummed fits to the EEC, applying *R-matching* and *modified R-matching* with renormalization scale factor $f = 1$. The fit range was restricted to the angular region $90^\circ \leq \chi \leq 154.8^\circ$ for *R-matching* and $90^\circ \leq \chi \leq 162^\circ$ for *modified R-matching* according to the criteria discussed in Section IV.A. The *R-matching* case does not describe the data in the large angle region, $\chi \gtrsim 155^\circ$. Figure 9 shows the resulting $\alpha_s(M_Z^2)$ and χ^2_{dof} values as a function of f for *modified R-matching* with all four $\mathcal{O}(\alpha_s^2)$ calculations. The most significant features are that $f \gtrsim 0.2$ is needed to fit the data, and α_s varies slowly with f, resulting in a significantly smaller scale uncertainty than in the $\mathcal{O}(\alpha_s^2)$ case, as expected. Once again, large differences in α_s are apparent between the matched RSE, AB, FK and KN calculations. The results for *R-matching*, shown in Fig. 10, are qualitatively similar, but are found to have a slightly larger variation of α_s with f than that from *modified R-matching*, probably due to the neglect of the sub-leading term in the exponentiation (Section I).

To quote a single value of α_s for each matched calculation we adopt the same procedure as in the $\mathcal{O}(\alpha_s^2)$ fits but use the range $1/4 \leq f \leq 4$, where the lower

bound ensures that fit qualities remain reasonable.† This is the same f range that we considered in our α_s measurement from jet rates using resummed calculations [2]. The results are shown in Table 1. We note that in each case the matched fit yields systematically larger α_s values than the $\mathcal{O}(\alpha_s^2)$ fit, and that the *modified R-matching* results are systematically larger than the *R-matching* results. Taking the average over all four calculations as before, and averaging over both matching schemes, we obtain

$$\alpha_s(M_Z^2) = 0.130 \pm 0.002(stat.) \begin{matrix} +0.002 \\ -0.003 \end{matrix} (syst.) \pm 0.007(theory),$$

where the total theoretical uncertainty is the sum in quadrature of contributions from hadronization ($\pm$ 0.002), calculation ($\pm$ 0.005), scale ($\pm$ 0.002), and matching ($\pm$ 0.004) uncertainties. Here we included a matching uncertainty from the difference in α_s values between *R-matching* and *modified R-matching* as a contribution to the total theoretical uncertainty. It is interesting to note that the dominant uncertainty in this case arises from the discrepancies between the four $\mathcal{O}(\alpha_s^2)$ calculations, the scale uncertainty being even smaller than the total experimental error. Resolution of this discrepancy between calculations would potentially yield, therefore, a precise measurement of α_s in e^+e^- annihilation at the Z^0 resonance. The above result is in agreement with that from the $\mathcal{O}(\alpha_s^2)$ fits

† For *R-matching*, scale factors as small as $f \sim 0.06$ are allowed by the quality of the fits to the data (Fig. 10(b)). However, Fig. 10(a) shows that the change in $\alpha_s(M_Z^2)$ between $f = 1/4$ and $f = 0.06$ is at most 0.002 in magnitude (FK calculation). The change in the mean $\alpha_s(M_Z^2)$, averaging over all four calculations, is smaller than 0.0004, which is negligible compared with statistical errors. Therefore, extending the f range down to 0.06 does not affect our final α_s result, and we use the range $1/4 \leq f \leq 4$ for consistency with our jet rates analysis [2].

to the EEC within experimental errors, and with the result from the $\mathcal{O}(\alpha_s^2)$ fits to the $AEEC$ within the combined experimental errors and theoretical uncertainties.

V. SUMMARY

We have measured energy-energy correlations and their asymmetry in hadronic Z^0 decays and compared our corrected data with four $\mathcal{O}(\alpha_s^2)$ perturbative QCD calculations in order to extract α_s. We have also combined these calculations with a resummed calculation using two matching schemes and extracted α_s from the EEC. We obtained

$$\alpha_s(M_Z^2) = 0.127 \begin{matrix}+0.002 \\ -0.003\end{matrix}(exp.) \pm 0.013(theory) \text{ from } EEC \ (\mathcal{O}(\alpha_s^2)),$$

$$\alpha_s(M_Z^2) = 0.116 \pm 0.005(exp.) \pm 0.006(theory) \text{ from } AEEC \ (\mathcal{O}(\alpha_s^2)),$$

$$\alpha_s(M_Z^2) = 0.130 \begin{matrix}+0.003 \\ -0.004\end{matrix}(exp.) \pm 0.007(theory) \text{ from } EEC \ (\mathcal{O}(\alpha_s^2) + \text{resummed}),$$

where the experimental error is the sum in quadrature of the statistical and systematic errors. Note that all experimental errors and theoretical uncertainties are highly correlated. These α_s values correspond to $\Lambda_{\overline{MS}} \simeq 360$MeV, 200MeV and 420MeV, respectively. The renormalization scale ambiguity dominates the uncertainty in the first case, but in the second and third cases it is dominated by the discrepancy between the four $\mathcal{O}(\alpha_s^2)$ calculations. In the third case there is also a large uncertainty from matching the $\mathcal{O}(\alpha_s^2)$ and resummed calculations. The renormalization scale dependence of the $\mathcal{O}(\alpha_s^2)$ results, as well as the reduction of renormalization scale sensitivity and the increase in measured α_s with the application of resummed calculations, is similar to that reported in our measurement of α_s from jet rates [2]. The results using $\mathcal{O}(\alpha_s^2)$ and resummed+$\mathcal{O}(\alpha_s^2)$ calculations are also consistent within experimental errors

with similar analyses by the LEP experiments [9–11,16,18–22]. Taking an unweighted average over all three results we obtain: $\alpha_s(M_Z^2) = 0.124^{+0.003}_{-0.004}(exp.) \pm 0.009(theory)$, corresponding to $\Lambda_{\overline{MS}} = 317^{+48}_{-64}(exp.) \pm 144(theory)$ MeV.

Acknowledgements

We thank the personnel of the SLAC accelerator department and the technical staffs of our collaborating institutions for their efforts which resulted in the successful operation of the SLC and the SLD. We thank S.J. Brodsky, S.D. Ellis, J.W. Gary, G. Kramer and G. Turnock for helpful comments relating to this analysis.

Table 1: $\alpha_s(M_Z^2)$ and scale uncertainties from $\mathcal{O}(\alpha_s^2)$ QCD fits to the EEC and the $AEEC$, and from $\mathcal{O}(\alpha_s^2)$+resummed fits to the EEC.

QCD calculation	$\mathcal{O}(\alpha_s^2)$ fits				$\mathcal{O}(\alpha_s^2)$+resummed fits			
	EEC		$AEEC$		EEC			
					mod. R-matching		R-matching	
	$\alpha_s(M_Z^2)$	Scale uncertainty	$\alpha_s(M_Z^2)$	Scale uncertainty	$\alpha_s(M_Z^2)$	Scale uncertainty	$\alpha_s(M_Z^2)$	Scale uncertainty
AB	0.132	$\pm$ 0.011	0.114	$\pm$ 0.004	0.138	$\pm$ 0.001	0.130	$\pm$ 0.003
FK	0.119	$\pm$ 0.013	0.113	$\pm$ 0.003	0.127	$\pm$ 0.002	0.120	$\pm$ 0.004
KN	0.125	$\pm$ 0.012	0.114	$\pm$ 0.004	0.133	$\pm$ 0.001	0.124	$\pm$ 0.004
RSE	0.133	$\pm$ 0.011	0.124	$\pm$ 0.008	0.140	$\pm$ 0.001	0.130	$\pm$ 0.003

Table 2: Summary of estimated experimental systematic errors on $\alpha_s(M_Z^2)$ for the EEC and $AEEC$.

Source	EEC	$AEEC$
Tracking		
Track selection	$^{+0.0006}_{-0.0011}$	$^{+0.0006}_{-0.0011}$
Tracking efficiency	+0.0006	+0.0013
Momentum resolution	-0.0010	-0.0003
Event selection		
Multiplicity cut	+0.0019	$^{+0.0026}_{-0.0023}$
Fiducial cut	$^{+0.0009}_{-0.0028}$	$^{+0.0023}_{-0.0024}$
Monte Carlo statistics	$\pm$0.0003	$\pm$0.0007
Total experimental error	$^{+0.0023}_{-0.0032}$	$^{+0.0040}_{-0.0042}$

REFERENCES

1. H. Fritzsch, M. Gell-Mann and H. Leutwyler, Phys. Lett. **B47** (1973) 365, D.J. Gross and F. Wilczek, Phys. Rev. Lett. **30** (1973) 1343, H.D. Politzer, Phys. Rev. Lett. **30** (1973) 1346.
2. SLD Collab., K. Abe *et al.*, Phys. Rev. Lett. **71** (1993) 2528.
3. C.L. Basham *et al.*, Phys. Rev. Lett. **41** (1978) 1585, Phys. Rev. **D17** (1978) 2298, Phys. Rev. **D19** (1979) 2018.
4. D.G. Richards, W.J. Stirling and S.D. Ellis, Nucl. Phys. **B229** (1983) 317.
5. A. Ali and F. Barreiro, Nucl. Phys. **B236** (1984) 269.
6. N.K. Falck and G. Kramer, Z. Phys. **C42** (1989) 459.
7. Z. Kunszt and P. Nason, Z Physics at LEP 1, CERN Report CERN 89–08, Vol. 1 eds. G. Altarelli, R. Kleiss and C. Verzegnassi, p. 373.
8. Review of Particle Properties, K. Hikasa *et al.*, Phys. Rev. **D45** (1992) III.54.
9. L3 Collab., B. Adeva *et al.*, Phys. Lett. **B257** (1991) 469.
10. ALEPH Collab., D. Decamp *et al.*, Phys. Lett. **B257** (1991) 479.
11. OPAL Collab., P.D. Acton *et al.*, Phys. Lett. **B276** (1992) 547.
12. S. Catani *et al.*, Nucl. Phys. **B407** (1993) 3.
13. G. Turnock, Cambridge Preprint Cavendish–HEP–92/3 (1992).
14. R. Fiore, *et al.*, Phys. Lett. **B294** (1992) 431.
15. J.C. Collins and D.E. Soper, Nucl. Phys. **B193** (1981) 381.
16. OPAL Collab., P.D. Acton *et al.*, Z. Phys. **C59** (1993) 1.
17. B.R. Webber, CERN–TH–6706–92 (1992).
18. DELPHI Collab., P. Abreu *et al.*, Phys. Lett. **B252** (1990) 149.
19. DELPHI Collab., P. Abreu *et al.*, Z. Phys. **C59** (1993) 21.
20. OPAL Collab., M.Z. Akrawy *et al.*, Phys. Lett. **B252** (1990) 159.
21. ALEPH Collab., D. Decamp *et al.*, Phys. Lett. **B284** (1992) 163.
22. L3 Collab., O. Adriani *et al.*, Phys. Lett. **B284** (1992) 471.
23. SLD Design Report, SLAC Report 273 (1984).
24. C.J.S. Damerell *et al.*, Nucl. Inst. Meth. **A288** (1990) 288.
25. D. Axen *et al.*, Nucl. Inst. Meth. **A328** (1993) 472.
26. A.C. Benvenuti *et al.*, Nucl. Instr. Meth. **A290** (1990) 353.
27. E. Farhi, Phys. Rev. Lett. **39** (1977) 1587.

28. T. Sjöstrand and M. Bengtsson, Comp. Phys. Comm. **43** (1987) 367.
29. G. Marchesini *et al.*, Comp. Phys. Commun. **67** (1992) 465.
30. S.L. Linn *et al.*, CERN–DD/78/12 (1978).
31. TASSO Collab, W. Braunschweig *et al.*, Z. Phys., **C41** (1988) 359;
P. N. Burrows, Z. Phys. **C41** (1988) 375.
32. OPAL Collab., M.Z. Akrawy *et al.*, Z. Phys. **C47** (1990) 505.
33. B.R. Webber, private communications.
34. The criteria for convergence are discussed in: P.N. Burrows and H. Masuda,
SLAC–PUB–6394 (1993); to appear in Z. Phys. C.

Figure captions

Fig. 1: The measured (a) EEC and (b) $AEEC$ (points with error bars) compared with the JETSET (solid histogram) and HERWIG (dashed histogram) Monte Carlo simulations.

Fig. 2: EEC results: (a) SLD data fully corrected for detector and hadronization effects using JETSET (see text). (b) Detector correction factors from JETSET (solid line) and HERWIG (dashed line). (c) Hadronization correction factors from JETSET (solid line with band) and HERWIG (dashed line). The width of the band in (c) represents the correction uncertainty calculated from JETSET (see text). Also shown as histograms in (a) are results of the fits of all four $\mathcal{O}(\alpha_s^2)$ calculations at $f = 1$ to the fully corrected EEC (see text). The fit range is indicated by vertical lines.

Fig. 3: $AEEC$ results: As Fig. 2, but (b) and (c) show the sizes of effective correction factors (see text).

Fig. 4: (a) $\alpha_s(M_Z^2)$ and (b) χ^2_{dof} from $\mathcal{O}(\alpha_s^2)$ QCD fits to the EEC as a function of renormalization scale factor f (see text). The width of the band indicates the size of statistical errors, shown for the KN fit only. The vertical lines indicate the range used in the average (see text).

Fig. 5: As Fig. 4, but for the $AEEC$.

Fig. 6: Results of the fits of KN $\mathcal{O}(\alpha_s^2)$ and matched (*modified R-matching*) calculations to the fully corrected EEC. The dots represent the data points. The fit range is indicated by vertical lines. The solid histogram represents the fit of the matched calculation ($f = 1$), the dashed histogram represents the fit of the $\mathcal{O}(\alpha_s^2)$ calculation ($f = 1$), and the dotted histogram represents the fit of the $\mathcal{O}(\alpha_s^2)$ calculation ($f = 0.0033$).

Fig. 7: (a) $\alpha_s(M_Z^2)$ and (b) χ^2_{dof} from fits to the EEC using $\mathcal{O}(\alpha_s^2)$ and matched (*modified R-matching*) calculations (see text).

Fig. 8: Results of the fits of the KN $\mathcal{O}(\alpha_s^2)$+resummed calculation to the fully corrected EEC. The dots represent the data points. The fit ranges are indicated by the vertical lines. The solid histogram (dotted histogram) represents the fit at $f = 1$ using *modified R-matching* (*R-matching*).

Fig. 9: (a) $\alpha_s(M_Z^2)$ and (b) χ^2_{dof} from fits to the EEC using the resummed calculation combined with each of the four $\mathcal{O}(\alpha_s^2)$ calculations using the *modified*

R-matching scheme. The width of the band indicates the size of statistical errors, shown for the KN fit only. The vertical lines indicate the range used in the average (see text).

Fig. 10: As Fig. 9, but for the *R-matching* scheme.

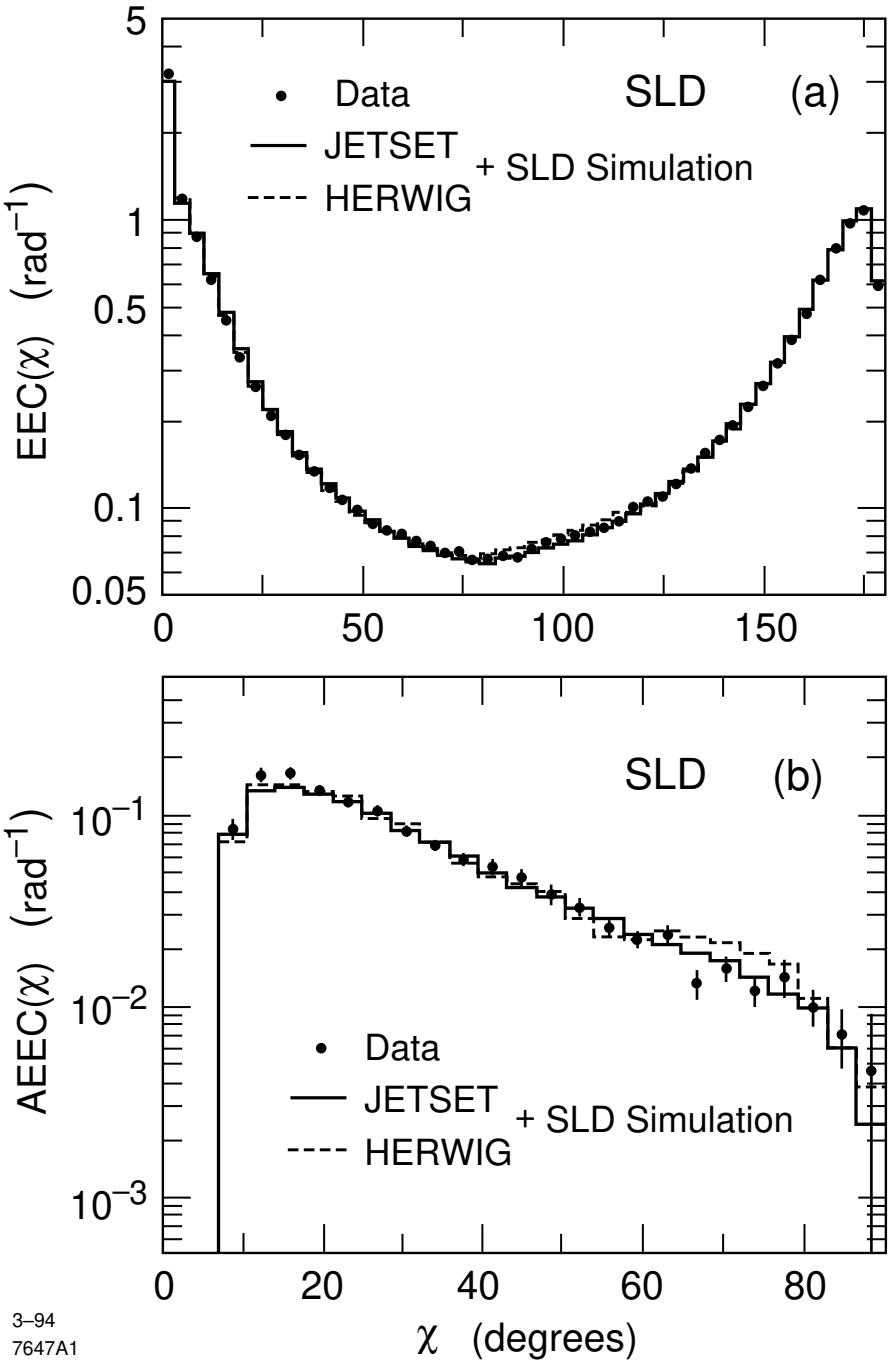

Fig. 1

Figure 1

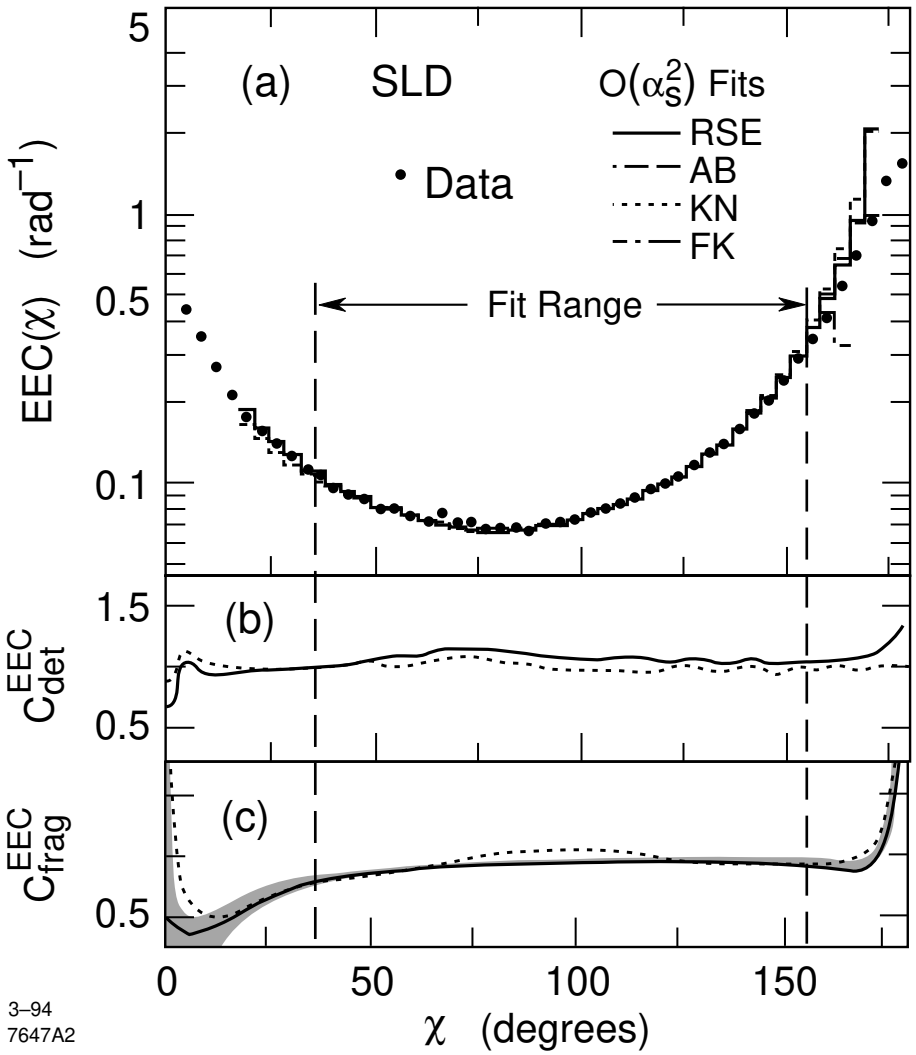

Fig. 2

Figure 2

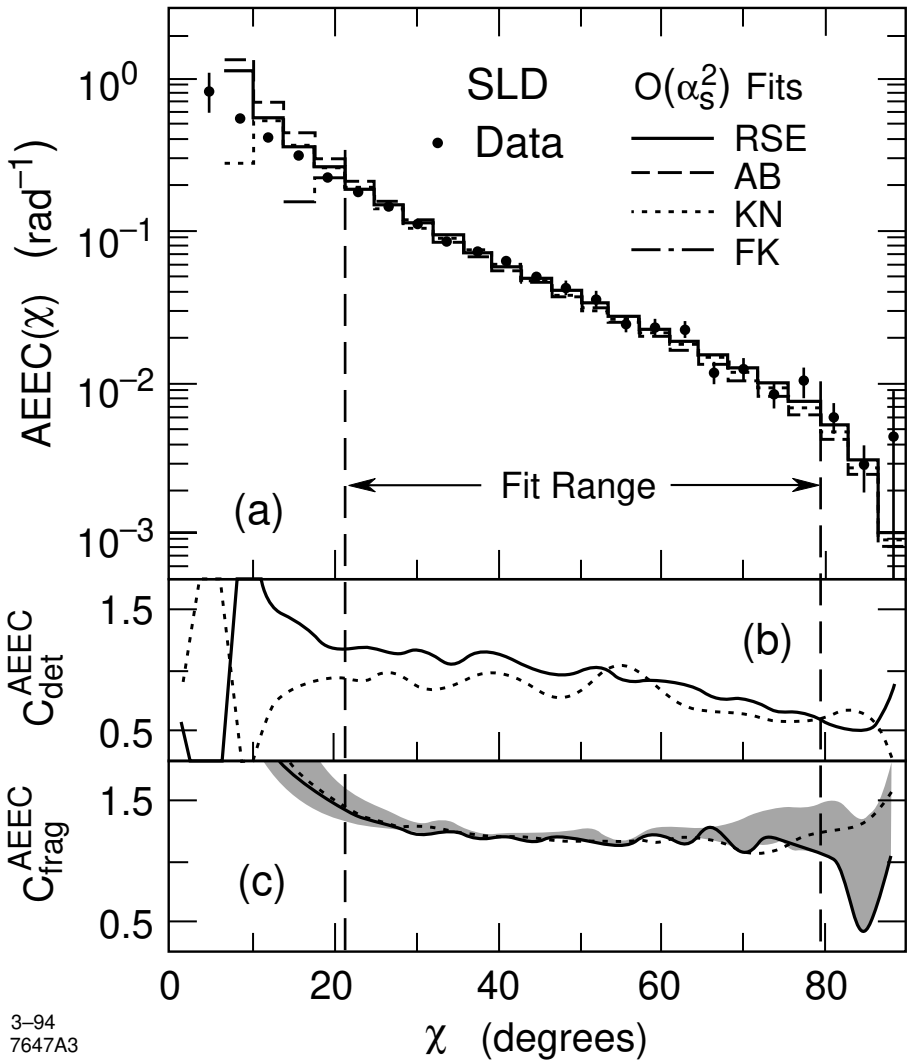

Fig. 3

Figure 3

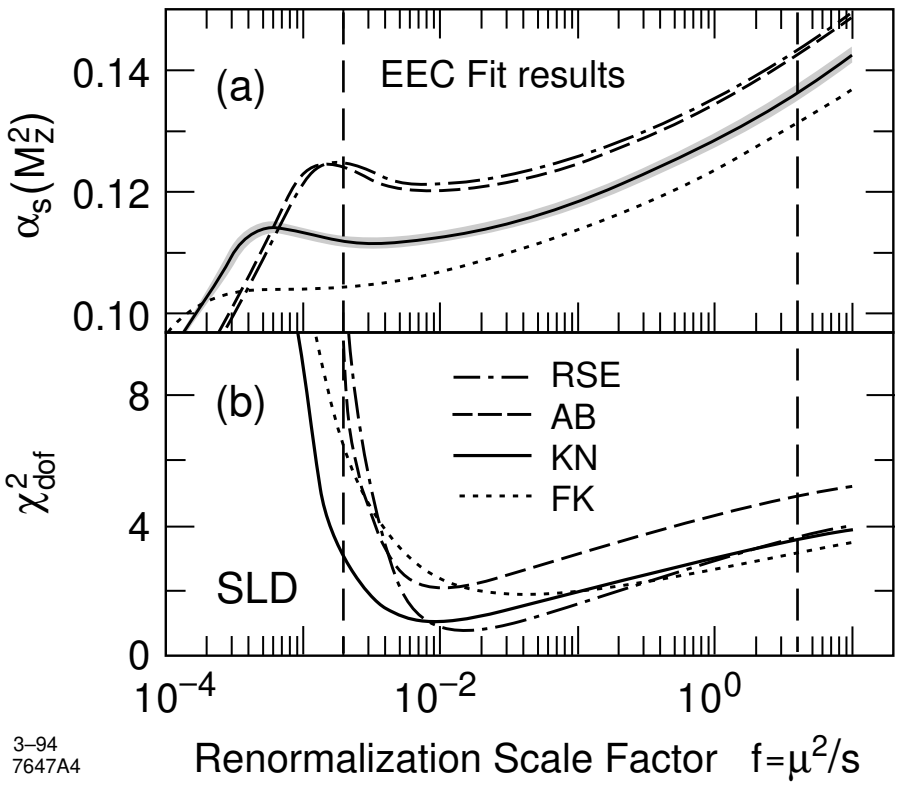

Fig. 4

Figure 4

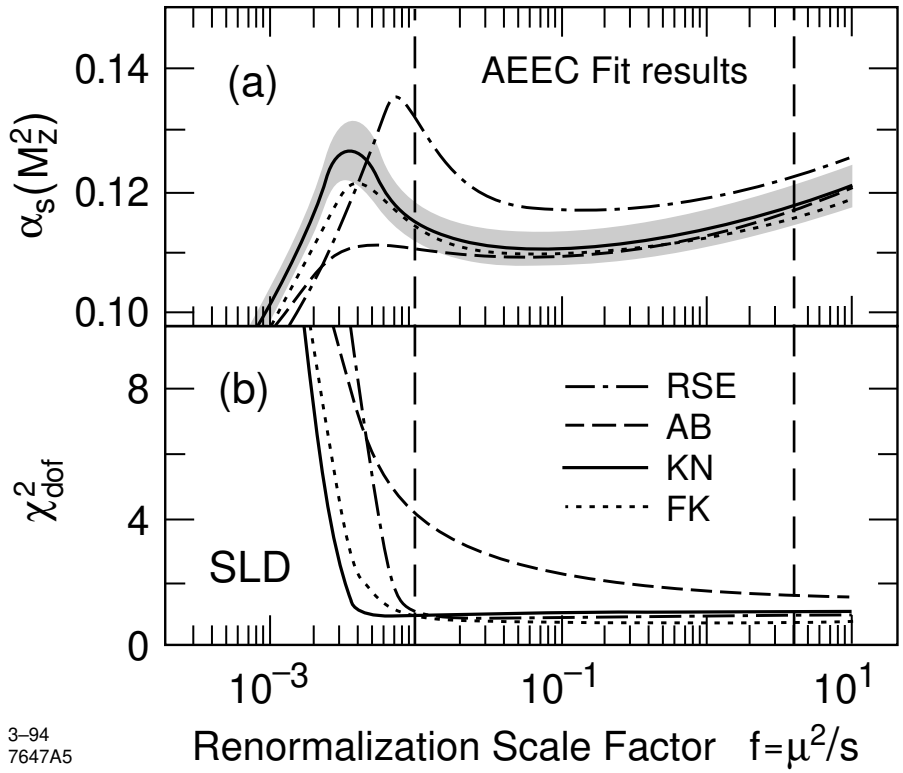
0.14
0.12
0.10
(a)
AEEC Fit results
$\alpha_s(M_Z^2)$
8
4
0
(b)
RSE
AB
KN
FK
SLD
χ^2_{dof}
10^{-3}
10^{-1}
10^{1}
Renormalization Scale Factor f=μ^2/s
3–94
7647A5

Figure 5

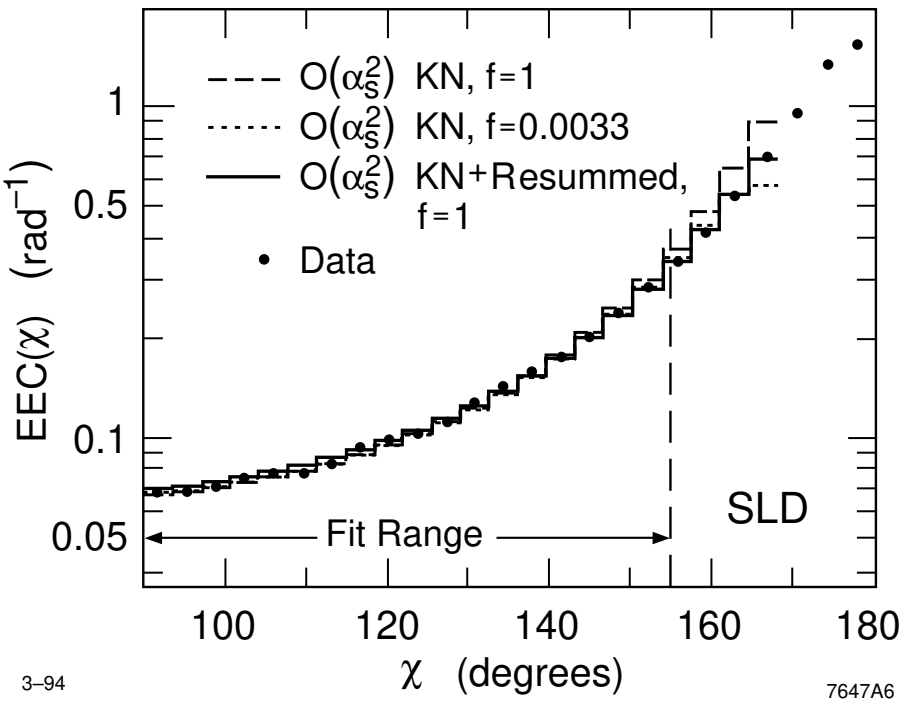

Fig. 6

Figure 6

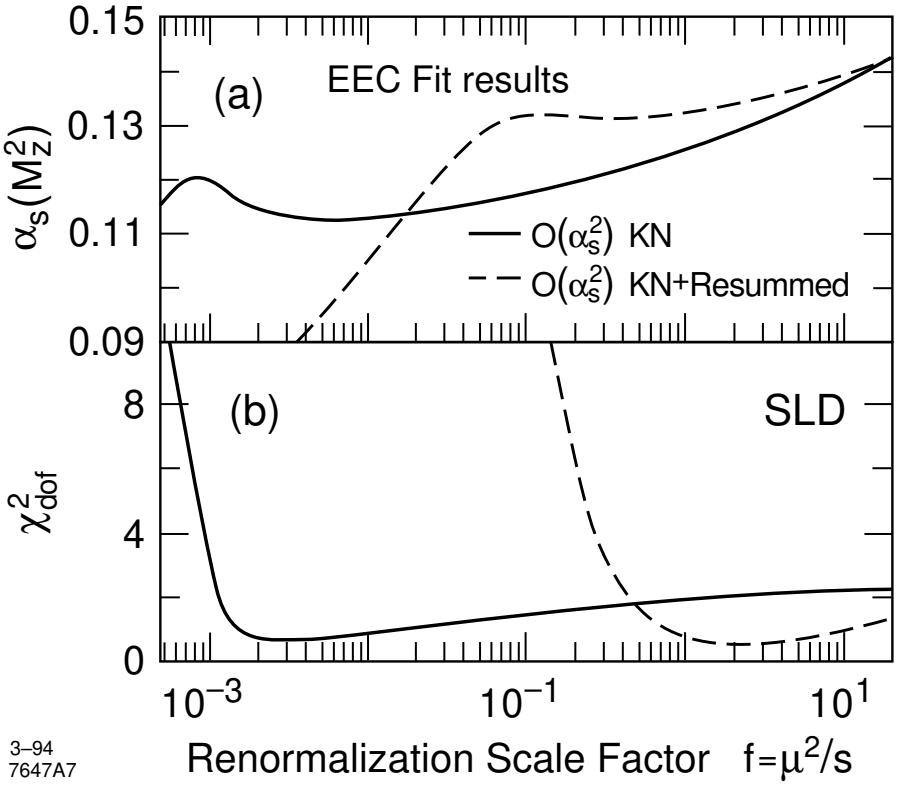

Fig. 7

Figure 7

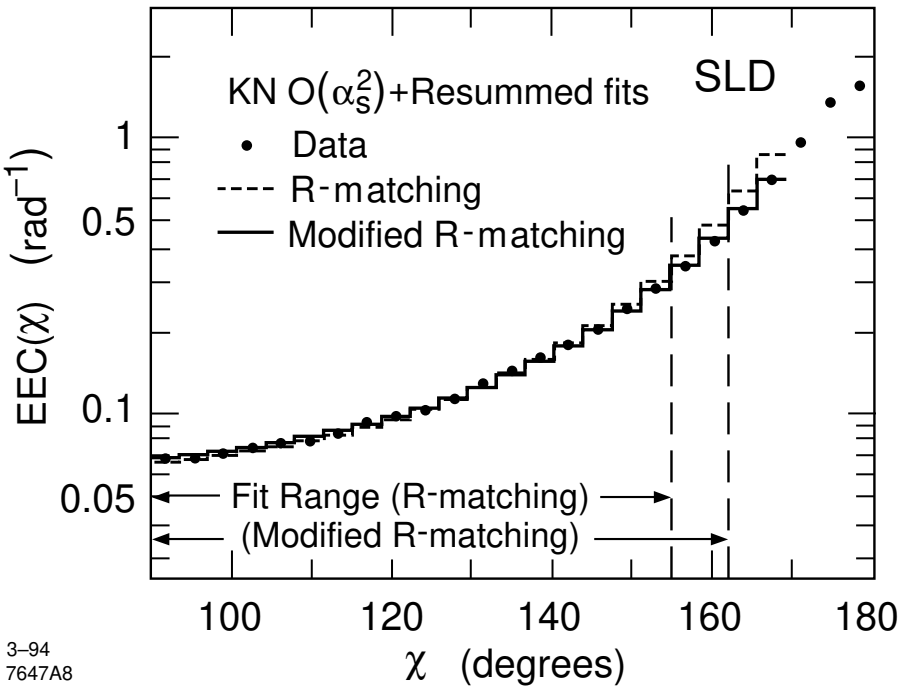

Fig. 8

Figure 8

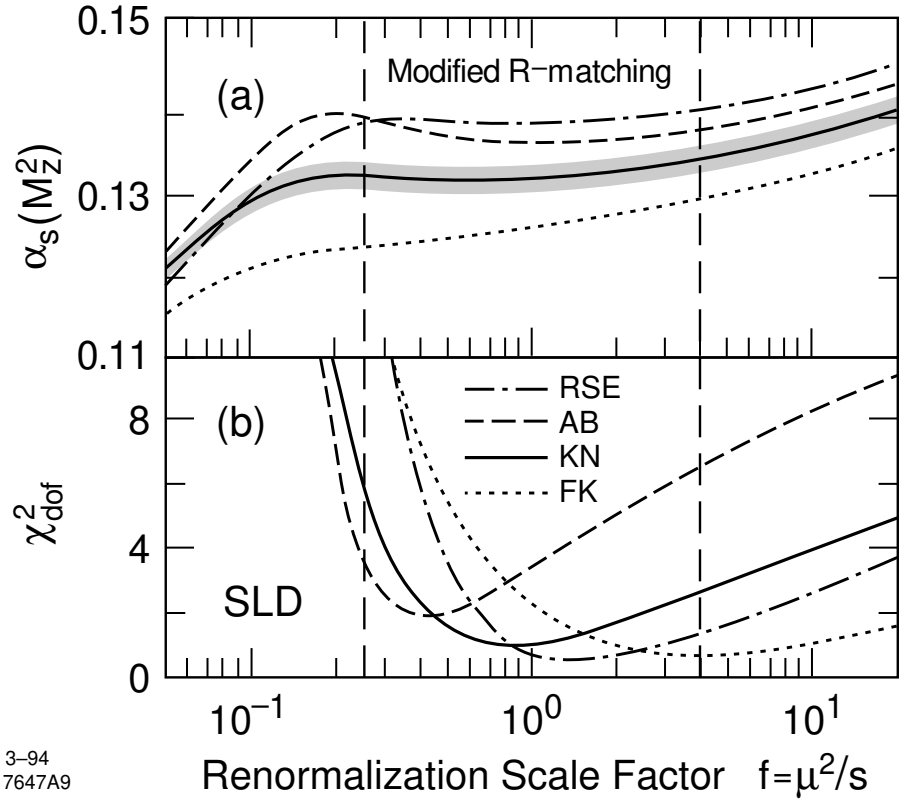

Fig. 9

Figure 9

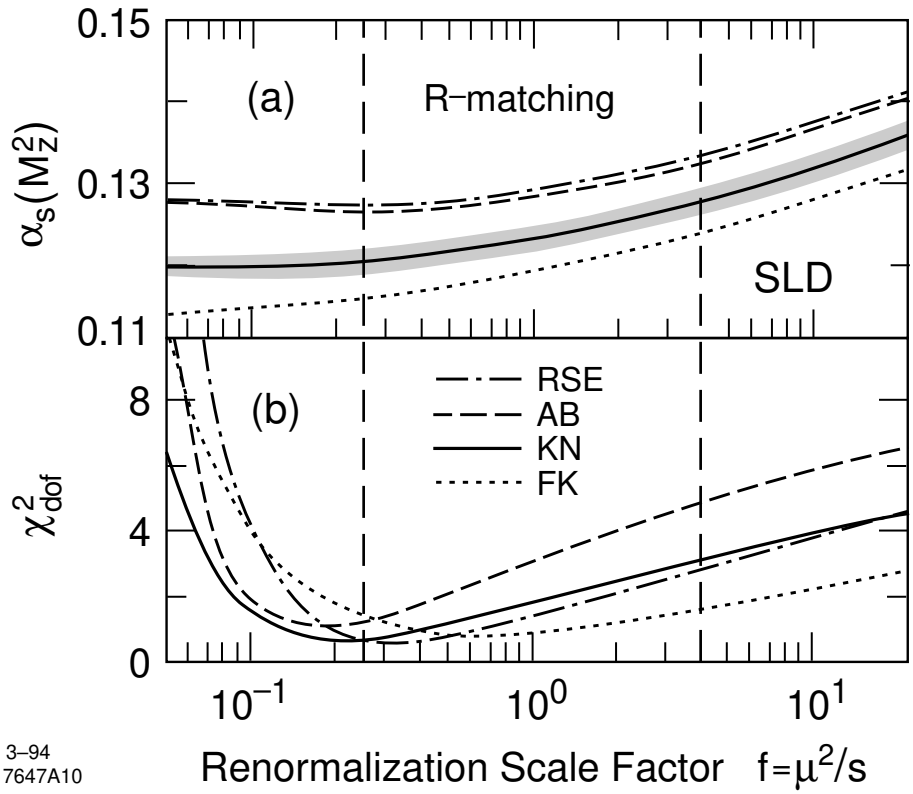

Fig. 10

Figure 10